

# Grain Boundaries in the Cuprate Superconductors: Tapes and Tunneling Spectroscopy

P Chaudhari and Heejae Shim

Brookhaven National Laboratory, Upton NY 11973 USA

Email: [chaudhari@bnl.gov](mailto:chaudhari@bnl.gov)

## **Abstract**

Grain boundaries in the high temperature superconducting cuprates have played a central role in their development for practical applications and fundamental understanding of the nature of superconductivity in these materials. Tapes for energy use, SQUIDS, symmetry of the wave function, Qbits, applications related to the AC Josephson effect, and tunneling spectroscopy are some areas of current research. In this brief note, the authors summarize what we know about what limits the critical current densities of tapes and suggest a few experiments to further understand these limits to critical current densities and, secondly, the use of grain boundary to do tunneling spectroscopy in optimally doped  $\text{La}_{1.84}\text{Sr}_{0.16}\text{CuO}_4$  (LSCO). This includes new data and comparisons with theory and experiments. The background material and review was presented at the EUCAS 09 in Dresden, as one of the plenary talks and is available from the authors.

Keywords: Superconducting tapes, Cuprate superconductors, High Tc films, Tunneling phenomena

PACS: 84.71.Mn, 74.72.-h, 74.78.Bz, 74.50.+r

## **1. Tapes**

The application defining curve, critical current density of a grain boundary versus the misorientation angle of the boundary,  $J_c$  vs.  $\theta_{gb}$  clearly pointed to the reality that to produce high critical current density tapes the misorientation angle, between the grain boundaries had to approach zero [1]. Many techniques

were tried and currently there are two competing methods both of which rely on textured substrates, suitably buffered, to produce YBCO tapes with misorientation angles of less than  $8^\circ$ . These are RAbITS [2] and IBAD [3]. It is not our intent to review where we stand on these tapes from a commercial aspect but to review in a succinct way some key experiments that tell us what experiments to do next in order to improve the critical current densities to even larger values in tapes. We apologize to the many colleagues whose fine work we will not be able to reference here but have described in the presentation as we focus on a few critical experiments relevant to this paper.

Although it was always understood that in low angle grain boundaries the critical current densities were limited by discrete dislocation that define such boundaries and not by Josephson coupling it was not until the experiments carried out by Diaz et al [4] and Gurevich et al [5] that it became clear that grain boundaries behave as channels for the movement of Abrikosov and Josephson vortices depending upon the misorientation angle and applied magnetic fields. These experiments raise the question: why do discrete and well separated dislocations that have a core of the order of the lattice parameter, enable the motion of vortices along the grain boundaries? These same dislocations provide very effective pinning in epitaxial films of YBCO [6].

The answer, we believe, comes from three experiments carried out by transmission electron microscopy of the study of Ca (or O) doping of low angle boundaries. In the first of these three experiments Schofield et al [7] showed, using electron holography in a transmission electron microscope that there is a negative electric potential around the core of a dislocation that extends to approximately 1.5 nm and is more elongated along the grain boundary plane than perpendicular to it. On doping with Ca, the potential decreases as does the range to approximately half the value observed in the undoped sample. Edge dislocations arrays are known to have large biaxial strain fields that alternate in sign along the length of array. Kile et al [8] have proposed and verified experimentally that these strain fields are sufficiently strong to change the distribution of ions along the array. The authors mapped out the Ca and O distribution along the dislocation array using energy loss spectroscopy in a scanning transmission microscope and a probe size of 0.1 nm. The results were in qualitative agreement with their calculations. A similar conclusion was reached by Song et al [9] where they studied the distribution of Ca ions along the length of the boundary.

These findings suggest a strategy to modify the properties of the edge dislocations in the cuprate superconductors without modifying the properties of the film surrounding the boundary. Dope the region around the core of a dislocation by using the pipe diffusion properties of dislocation cores. One approach may be to use gas phase chemistry, whether the gas is ionized or not, to drive selected ions to diffuse down the dislocation pipes. For example, ozone can provide a source of oxygen.

Feldman et al [10] have reported some surprising data which exceeds the limit generally defined by the exponential dependence of the critical current densities by factors of 4-6 when the grain boundaries meander rather than lie in a straight plane perpendicular to the film plane. The authors attribute this to three factors: area of the grain boundary is larger than estimated, vortex cutting, and vortex pinning. In a simple experiment the authors show that underestimating the area can contribute but cannot explain their results. We believe these results raise interesting questions, which can be answered by three straightforward bicrystal experiments. The first of these experiments has already been done by Feldman et al [10] but needs more data.

Here are the three proposed experiments: In the Feldman et al [10] paper they describe a bicrystal experiment in which the direction of current flow is changed by an angle  $\alpha$ , measured from the perpendicular of the a-b plane of the bicrystal grain boundary (Fig. 1(a)). If the critical current density is determined by tunneling the measured value will scale as  $\cos(\alpha)$ , as expected from a simple area argument. If, however, the critical current is determined by a Lorentz force on the vortices the dependence should scale as  $\cos^2(\alpha)$ , provided  $J_{gb} \leq J_{film}$ .

A symmetrical low angle tilt boundary has a well defined dislocation array. However, if the plane of the boundary is no longer symmetrical, additional dislocations are introduced and the strain field changes markedly and the energy of the boundary increases (Fig. 1(b)). It is not clear if this will increase or decrease the critical current density of the boundary nor is it clear if the transition from Abrikosov to the mixed Abrikosov- Josephson vortex is changed. A bicrystal experiment with asymmetrical boundaries but fixed tilt angle can answer these questions.

Finally, the cuprates are known to have d-wave symmetry near grain boundaries. [11] If the low angle grain boundary meanders and Josephson coupling across the boundary is strong, even though it does not determine the critical current density, it can introduce d-wave induced vortices, as shown in Fig. 1(c). These vortices differ from the Abrikosov and Josephson vortices not only in the value of the flux quantum but, more significantly, from the critical current density perspective by the fact that they are spatially locked to the grain boundary topology. Hence, any Lorentz force driven mobile vortex is likely to encounter a significant barrier.

In summary, we should not abandon our goal of fabricating cuprate superconducting tapes on single crystal metallic substrates. If we can develop single crystal tapes it would help not only in the field of high temperature superconductivity but with different buffer layer provide for inexpensive high efficiency silicon solar cells We believe this is a grand challenge for this decade in the field of Materials science.

An intriguing experimental result is the role of meandering grain boundaries, as described by Feldmann et al. This data needs to be confirmed. Assuming that it will be verified, it has led us to propose some

additional experiments to probe the origin of the critical current densities in meandering grain boundaries beyond the original tiling proposal put forward by Mannhart almost 22 years ago.

## 2. Tunneling Spectroscopy

We first provide a general rationale for the importance of tunneling, currents along the a-b plane vs. c-axis and the importance of the use of grain boundaries to carry out tunneling in LSCO. We present some data that underscores the ease with which grain boundary junctions can be formed by ozone annealing. We present some unpublished comparisons of the tunneling spectra obtained by Shim et al [12]. The new comparisons of the tunneling spectra are with both experimental and theoretical phonon density of states in  $\text{La}_{1.84}\text{Sr}_{0.16}\text{CuO}_4$  (LSCO) films. We then compare the tunneling data with inelastic neutron spectroscopy data of spin excitations. A more detailed background, rationale, and review were presented in the review talk at EUCAS 09. This review included some other important techniques used to understand the origin of the boson responsible for pairing.

Most tunneling studies have been carried out by scanning tunneling microscopy (STM). There are two recent articles covering both a review (STM) and a Colloquium on other tunneling methods [13 (a, b)]. The vast majority of the experiments have been carried out on surfaces in which the tunneling currents flow perpendicular to the CuO planes. A great deal has been learnt through the scanning probe techniques about the surfaces of the cuprates, about vortices, and electronic properties. Some of the scanning tunneling experiments have been a tour de force in instrumentation and control [14-16]. One of the experiments [14] carried out on Bi2212 reports data on conductance ( $dI/dV$ ) but also the derivative of the conductance data ( $d^2I/dV^2$ ). After correcting for spatial variations in the value of the gaps, these authors conclude, based on their second derivative, that there is electron-phonon interaction with a phonon of energy equal to 52 meV.

Break junctions, used first in conventional superconductors as in Nb-Sn [17], have been used extensively in the case of cuprate superconductor. We give two examples to show case their ability and limitations. Spectroscopy data obtained on Bi2212 break junctions, which can be fitted with a convolution of two d-wave superconductors show a single bosonic feature, which has been identified with a resonance spin excitation by Zasadzinski et al [18] around 35-43 meV. If, however, the tunneling current has a component along the a-b plane, as evidenced by a lack of good fit to c-axis tunneling geometry using the d-wave gap function, the tunneling spectra invariably show many boson features that match phonon spectra (see, for example Gonnelli et al [19]).

A novel tunnel junction in which the tunneling current flows along the a-b planes and tunnels across a barrier constructed by penetrating a Bi2212 single crystal by a wedge shaped single crystal of GaN shows

well define superconducting gap features and a large number of bosons that Shimada et al [20] attribute to phonons.

It is not clear to us what relationship exists between the spectra obtained by tunneling currents flowing along the c-axis and the a-b planes. This is particularly puzzling in the case of the sister compound of LSCO namely LBSCO, where Ba replaces Sr. In LBCO, superconductivity appears to show a sharp dip when the Ba concentration reaches 1/8, the remaining being La (1 and 7/8). It is now known experimentally that the superconducting transition temperature does not change along the CuO planes with Ba doping but rather the c-axis Josephson coupling between the CuO planes [21].

### 2.1. The case for grain boundaries as tunnel barriers

It has been shown by Winkler et al [22] and many subsequent investigators that there is a thin insulating barrier present at the grain boundaries. These boundaries are perpendicular to the a-b planes hence providing a natural and ideal geometry. The difficulty has been to control the transparency of the barrier and the variation of composition near the grain boundaries. Generally, the surfaces and grain boundaries are deficient in oxygen due to the following reaction:



This results in oxygen vacancies near the grain boundaries and surfaces and concomitant loss of carriers, generally resulting in a lower  $T_c$ .

Supplying controlled amount of O, for example, by ozone can offset this loss and produce a stoichiometric oxygen distribution. This can be achieved without affecting the bulk behavior for grain boundary diffusion rates are much greater than the film.

### 2.2. Why LSCO?

There are many important experimental reasons for choosing LSCO as the starting material: The  $T_c$  of the films can be varied by controlling the deposition conditions or varying the substrate [23]; the critical magnetic field required to drive the film normal is available in many laboratories. This is essential if we are to determine a reliable electron-boson interaction constant. LSCO can be doped both by Sr or interstitial oxygen and this is important for it enabled us to check the validity of our approach by first doping with Sr to reach the optimal  $T_c$  and then subsequently over doping with ozone to drive the sample to the over doped state where the  $T_c$  drops. If we now allow the sample to sit at room temperature the  $T_c$  should recover as the interstitial oxygen diffuses out through the grain boundary.

### 2.3. Experimental verification

In the following section we describe some of our recent results obtained on LSCO films. These films were prepared for us by Dr. Logvenov in Dr. Bozovic's group at this Laboratory using their molecular beam epitaxial system. In our experiment the grain boundary was comprised of two crystals each rotated by  $12^\circ$  about the c-axis to form a  $24^\circ$  tilt bicrystal grain boundary. The LSCO films, 104 nm thick, were deposited on these bicrystal substrates. We patterned these films lithographically to form 25  $\mu\text{m}$  wide junctions. The bicrystal junction was modified by annealing in ozone at  $125^\circ\text{C}$  for various times to drive in enough oxygen so that the sample was in the over doped state and then we measured the gap as a function of time. The schematic diagrams illustrate the process and the conductance curves measured over time are shown in Fig. 2. After annealing a well-defined gap appears in the conductance data. We now follow the evolution of this gap with time.

We note that the first anneal was done at 275 K for one day. We observed no change. Next we kept it at room temperature for another day. The value of the gap began to increase on the third day, accelerated, and then slowed with time. In order to avoid degradation of the film on annealing at room temperature in air we annealed them in a good vacuum for many days, as shown in Fig. 2.

Following this confirmation of our expectations on the over doped side of the optimal composition; we next started to add ozone to the as prepared samples, where we expect oxygen vacancies. The goal is to achieve a kinetically equilibrated oxygen distribution to reach a uniform oxygen distribution across the grain boundary. An experimental challenge but we believe it can be met based on the preceding results and the published information by Shim et al [12], thus opening the possibility of investigating the magnitude of strength of the electron-boson coupling constant experimentally and, equally important, follow the change in the strength of the coupling constant with composition. In brief, we will be able to identify all of the relevant parameters which give rise to superconductivity in LSCO.

### 2.4. Grain boundary tunneling

We show in Fig. 3 two conductance curves. The broad V-shaped curve is typical of the as prepared grain boundaries in LSCO thin films, whether by MBE or pulse laser deposition. With increasing ozone annealing at  $125^\circ\text{C}$  and rapid cooling to room temperature the broad V-shaped curves become narrow and develop shoulders till we develop a conductance curve with features in it. We then measure the conductance and its derivative as a function of temperature.

### 2.5. Comparison with experiment and theory --- phonons

We have already compared our data with the published Raman scattering data and concluded the features in our spectra are associated with phonons. In Fig 4 (a), we show the first-principles calculation of the phonon density of states by Giustino, Cohen, and Louie [24] and that of Shim et al [12]. We note the agreement is impressive, reinforcing our earlier conclusions that the features we observe are associated with phonons. We note that Giustino, Cohen, and Louie have already compared favorably their calculated values with the inelastic neutron scattering data of McQueeney et al [25].

Giustino, Cohen, and Louie [24] have also calculated the electron-phonon coupling constant from first principles calculations and based on that have concluded that  $T_c$  should be very small. It is clear that an experimental determination of the electron-phonon coupling constant needs to be made, given the agreement on the energy scale on the locations of the phonon density of states with the tunneling data.

## 2.6. Comparison with magnetic excitations

As magnetic excitations are ubiquitous in the cuprates, we thought it might be useful to compare our spectra with the dynamic susceptibility measured by inelastic neutron scattering data obtained by Vignolle et al [26].

This is shown in Fig. 4(b). This data is collected on a LSCO crystal of the same composition as our superconducting film and the 11.1 K tunneling data [12] is superimposed on the neutron data collected at 12 K.

The partition of the two data sets into two broad regions and the agreement of the positions of the peaks are noteworthy. This could be a fortuitous agreement or, alternatively, the phonon and spin excitations interact constructively to reinforce each other and their interaction with electrons. Generalized boson theories by Monthoux, Pines, and Lanzarich [27] treat phonons and magnetic excitations as linear additions. This may not be adequate. There may be cross terms associated with strong magnetoelastic effects.

If we assume the agreement between the tunneling and inelastic scattering is causal, the emphasis of our attempt to understand these fascinating materials moves from finding the pairing boson to one of understanding how phonons and spin excitations collectively enhance electron-boson interactions?

## 2.7. Conclusions

We have shown that grain boundaries in an optimally doped LSCO film can be modified by controlled ozone annealing for use in tunneling spectroscopy. We have observed multiple well defined boson peaks which, by comparison with published theoretical and experimental data, lead to the conclusions that the relevant bosons are phonons in LSCO films.

We believe, with further experimental refinement, we can use tunneling spectroscopy to map out the pairing mechanism in LSCO and ascertain which phonons give rise to higher  $T_c$ .

### **Acknowledgements**

The authors are grateful to BSA and BNL for financial support of this work.

## Reference

- [1] Dimos D, Chaudhari P and Mannhart J 1990 Phys. Rev. B **41** 4038
- [2] Goel A, Paranthaman M P and Schoop U 2004 Mater. Res. Soc. Bull. August 552
- [3] Iujima Y, Kakimoto K, Yamada Y, Izumi T, Saitoh T and Shiohara Y 2004 Mater. Res. Soc. Bull. August 564
- [4] Diaz A, Mechin L, Berghuis P and Evetts J E 1998 Phys. Rev. Lett. **80** 3855
- [5] Gurevich A, Rzchowski M S, Daniels G, Patnaik S, Hinaus B M, Carillo F, Tafuri F and Larbalestier D C 2002 Phys. Rev. Lett. **88** 097001
- [6] Dam B, Huijbregtse J M, Klaassen F C, Geest R C F van der, Doornbos G, Rector J H, Testa A M, Freisem S, Martinez J C, Stäuble-Pümpin B and Griessen R 1999 Nature **399** 438
- [7] Schofield M, Beleggia M, Zhu Y, Guth K and Jooss C 2004 Phys. Rev. Lett. **92** 195502
- [8] Klie R F, Buban J P, Varela M, Franceschetti A, Jooss C, Zhu Y, Browning N D, Pantelides S T and Pennycook S J 2005 Nature **435** 475
- [9] Song X, Daniels G, Feldmann D M, Gurevich A and Larbalestier D 2005 Nature Mater. **4** 470
- [10] Feldmann D M, Holesinger T G, Feenstra R, Cantoni C, Zhang W, Rupich M, Li X, Durrell J H, Gurevich A and Larbalestier D C 2007 J. Appl. Phys. **102** 083912
- [11] Tsuei C C and Kirtley J R 2000 Rev. Mod. Phys. **72** 969
- [12] Shim H, Chaudhari P, Logvenov G and Bozovic I 2008 Phys. Rev. Lett. **101** 247004
- [13] (a) Fischer Ø, Kugler M, Maggio-Aprile I, Berthod C and Renner C 2007 Rev. Mod. Phys. **79** 353  
(b) Kresin V Z and Wolf S A 2009 Rev. Mod. Phys. **81** 481
- [14] Lee J, Fugita K, McElroy K, Slezak J A, Wang M, Aiura Y, Bando H, Ishikado M, Masui T, Zhu J – X, Balatsky A V, Eisaki H, Uchida S and Davis J C 2006 Nature **442** 546
- [15] Boyer M C, Wise W D, Chatterjee K, Yi M, Kondo T, Takeuchi T, Ikuta H and Hudson E W 2007 Nature **3** 802
- [16] Gomes K K, Pasupathy A N, Pushp A, Ono S, Ando Y and Yazdani A 2007 Nature **447** 569
- [17] Moreland J and Ekin J W 1986 J. Appl. Phys. **58** 3888
- [18] Zasadzinski J F, Ozyuzer L, Coffey L, Gray K E, Hinks D G and Kendziora C 2006 Phys. Rev. Lett., **96** 017004
- [19] Gonnelli R S, Ummarino G A and Stepanov V A 1997 Physica C **282-287** 1473
- [20] Shimada D, Shiina Y, Mottate A, Ohyagi Y and Tsuda N 1995 Phys. Rev. B **51** 16495
- [21] Tranquada J M, Gu G D, Hucker M, Jie Q, Kang H –J, Klingeler R, Li Q, Tristan N, Wen J S, Xu G Y, Xu Z J, Zhou J and Zimmermann M V 2008 Phys. Rev. B **78** 174529
- [22] Winkler D, Zhang Y M, Nilsson P Å, Stepanov E A and Claeson T 1994 Phys. Rev. Lett. **72** 1260

- [23] Sato H, Tsukada A, Naito M and Matsuda A 2000 Phys. Rev. B **61** 12447
- [24] Giustino F, Cohen M L and Louie S G 2008 Nature **452** 7190
- [25] McQueeney R J, Sarrao J L, Pagliuso P G, Stephens P W and Osborn R 2001 Phys. Rev. Lett. **87** 077001
- [26] Vignolle B, Hayden S M, McMorrow D F, Rønnow H M, Lake B, Frost C D, Perring T G 2007 Nature Phys. **3** 163
- [27] Monthoux P, Pines D and Lonzarich G G 2007 Nature **456** 1177

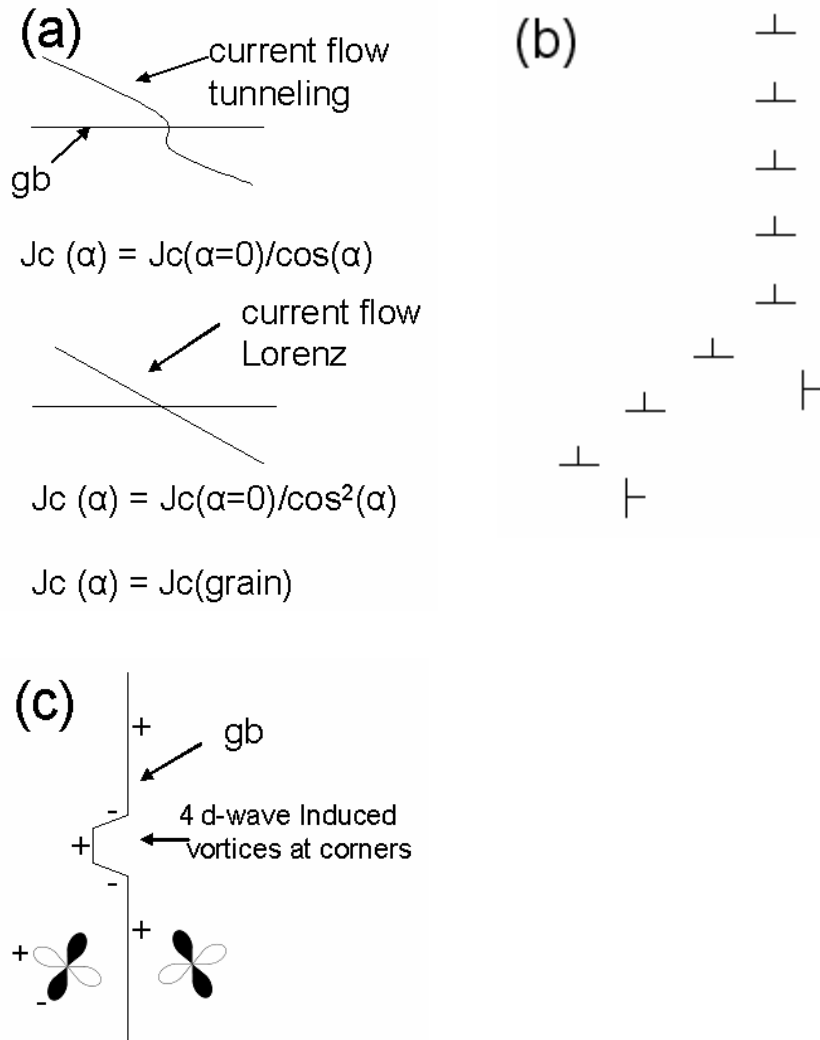


Figure 1. Schematic drawings of three experiments proposed in the text. (a) A sketch indicating current flow at an angle  $\alpha$  from the normal to the grain boundary plane marked gb, indicated as an horizontal line, see Feldmann et al [10]. (b) Edge dislocation array in a symmetrical grain boundary plane is the vertical array. Additional dislocations as the grain boundary plane meanders to the left. (c) A vertical grain boundary plane in which appreciable Josephson is present is tilted twice by a second phase as the grain boundary meanders and is bound around it. For an example see the photomicrograph in Feldmann et al [10]. Additional d-wave vortices are formed and pinned spatially.

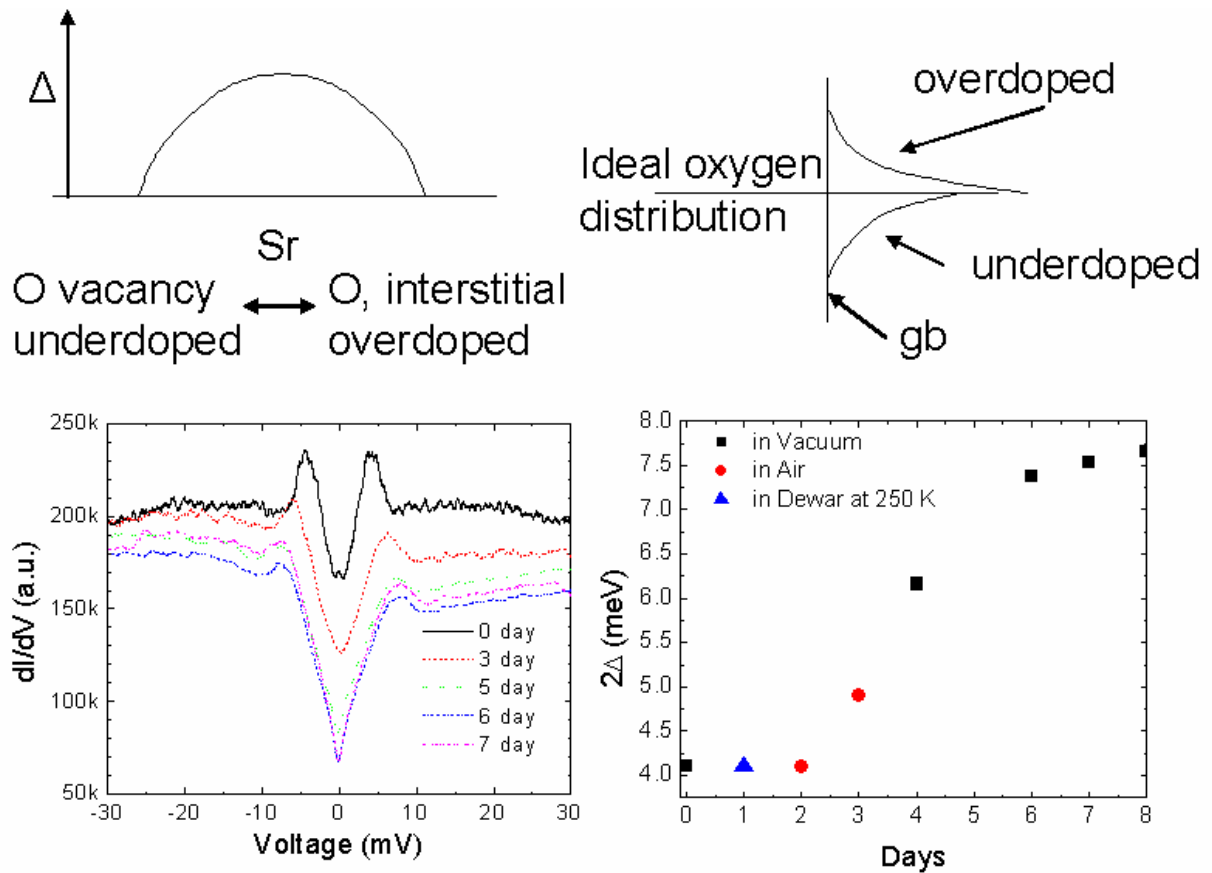


Figure 2. Schematic diagram on the left is of the superconducting gap value,  $\Delta$ , as a function of Sr doping. On the right is the spatial variation in oxygen doping across the grain boundary, gb for three different cases. The experimental conductance curve measured in an over doped sample as a function of time. The value of the measured gap is as a function of time.

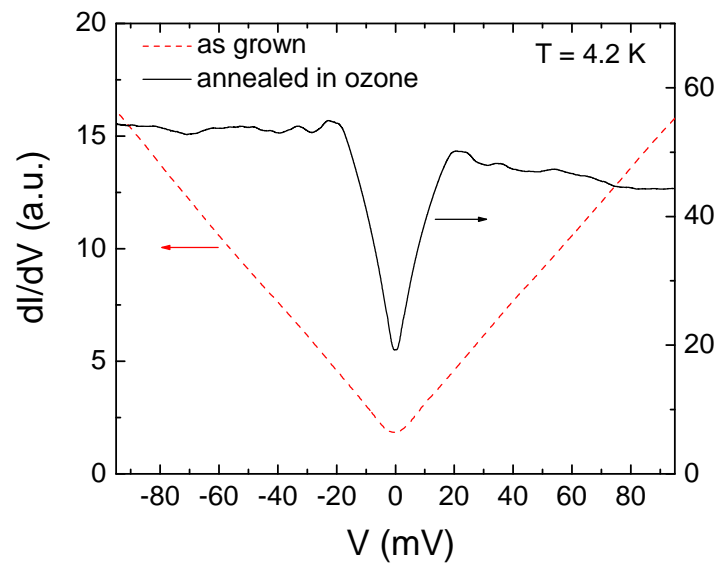


Figure 3. Conductance curve, broad and V-shaped, typically observed of an as received LSCO films deposited by MBE or PLD. With ozone annealing the V-shaped curve narrows, and the process continued till features of the type shown in the data appear.

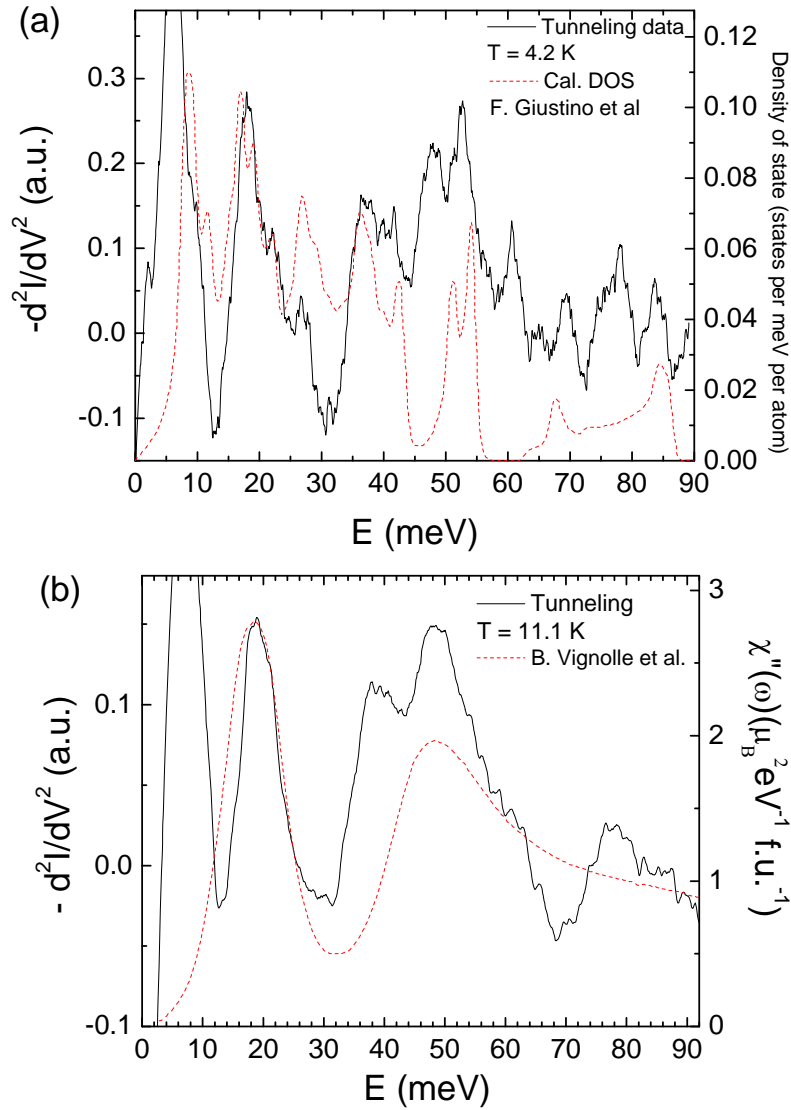


Figure 4. Comparison of the first derivative of the conductance curve multiplied by (-1) with theoretical phonon density of states and experimental inelastic neutron scattering. The data is from Reference Shim et al [12]. (a) The first-principles calculations are published by permission of the authors (Cohen and Louie) and Journal, Nature, from Guistino, Cohen, and Louie [24]. (b) A comparison with dynamic susceptibility obtained from inelastic neutron scattering by Vignolle et al [26]. The neutron data was collected at 12 K and the tunneling (Ref. 12) was measured at 11.1 K. The neutron data is with the permission of the Journal, Nature Physics.